Earthquakes and Structures, *Vol. 15, No. 5 (2018) 541-553*
DOI: https://doi.org/10.12989/eas.2018.15.5.541

Rapid evaluation of in-plane seismic capacity of masonry arch bridges through limit analysis

Marco Breccolotti[a], Laura Severini[b], Nicola Cavalagli*, Federico M. Bonfigli[c] and Vittorio Gusella[d]

Department of Civil and Environmental Engineering, University of Perugia, via Goffredo Duranti 93, 06125, Perugia, Italy

(Received June 28, 2018, Revised September 10, 2018, Accepted September 11, 2018)

Abstract. In this paper a limit analysis based procedure for the rapid evaluation of the in-plane seismic capacity of masonry arch bridges is carried out. Attention has been paid to the effect of the backfill on the collapse load. A parametric investigation has been performed by varying the rise/span ratio and the results have been compared with those obtained by finite element modelling. The comparison highlights the conservative feature of the proposed model in terms of ultimate loads and a good agreement in terms of collapse mechanisms.

Keywords: masonry bridges; limit analysis; seismic capacity; backfill

1. Introduction

The evaluation of existing masonry arch bridges represents an important task, related with human safety, social and economic issues but also with the conservation of architectural heritage. The oldest bridges still in service on vehicular, railways or pedestrian networks dated back to the medieval age or even earlier, while most of the worldwide current bridge stock was constructed in the 18th and the 19th century when no specific provisions were engaged for earthquake actions. Nevertheless, many of these bridges are located within seismic zones. Thus, it can be inferred that the assessment of these structures cannot be accomplished neglecting their vulnerability to in-plane and out-of-plane seismic actions.

In this paper, an analytical procedure based on the Limit Analysis (LA) is proposed in order to carry out fast evaluations of the in-plane seismic capacity of masonry arch bridges. In the context of definition of an intervention scale priority on the existing masonry bridge stock, these kinds of models could be used in order to achieve a rational funds management. The procedure aims at the determination of the in-plane seismic load multiplier and the corresponding collapse mechanism according to Heyman's hypotheses (1969). Thus no-tensile strength, infinite compressive strength and pure rotational failure mechanism are assumed for masonry. The arch is considered subjected to its self-weight, to the weight of the backfill and to the inertial loads induced by seismic action. The effects related to the presence of the backfill are considered in the calculus with the application of the active pressure, the seismic increment on the side from which the earthquake acts and the pressure exerted by the backfill on the opposite side as a consequence of the mechanism development. In particular, special attention has been deserved to the determination of this latter pressure, introducing a new model for the description of such effect that takes into account the shape of the collapse mechanism produced by the horizontal seismic action. For this reason, in the following, the effect related to this resistance will be called "*mechanism thrust*".

A parametric investigation has been carried out on arches with different rise/span ratios by using both the proposed procedure and a numerical Finite Element approach, in order to compare the results in terms of collapse load and kinematic mechanism. The FE model consists of the bridge structural parts and the surrounding soil, each of them characterized by non-linear constitutive materials, able to describe the structural response obtaining a consistent estimation of the collapse conditions.

2. Literature review

In the last decades the research effort to set up analytical, numerical and experimental procedures to assess the aging masonry arch bridges still in service along the existing road and railway networks increased continuously and a recent literature review has been published by Sarhosis *et al.* (2016). Among the analytical procedures several major contributions can be cited. De Santis and de Felice (2014) proposed a fiber beam-based methodology to study the dynamic behaviour of masonry arches and arch bridges capable of describing both the non-linear material properties and the seismic action. Da Porto *et al.* (2016)

*Corresponding author, Ph.D.
E-mail: nicola.cavalagli@unipg.it
[a]Ph.D.
E-mail: marco.breccolotti@unipg.it
[b]Ph.D.
E-mail: laura.severini@unipg.it
[c]Ph.D.
E-mail: federico.bonfigli@unipg.it
[c]Professor
E-mail: vittorio.gusella@unipg.it

Copyright © 2018 Techno-Press, Ltd.
http://www.techno-press.com/journals/eas&subpage=7 ISSN: 2092-7614 (Print), 2092-7622 (Online)

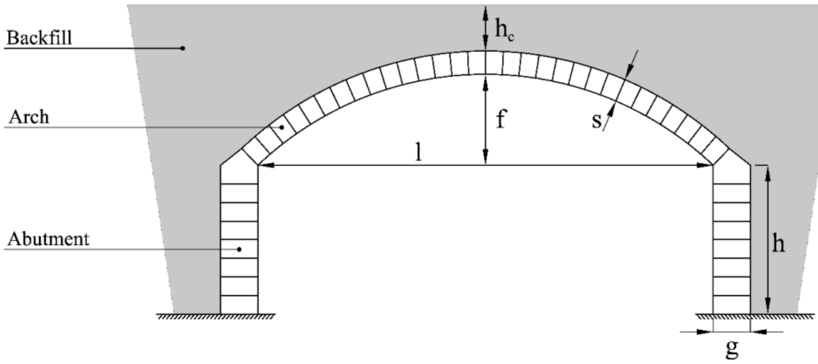

Fig. 1 Nomenclature and geometry of the masonry arch bridge

carried out a parametric study on the seismic capacity of masonry arch railway bridges through a procedure based on limit analysis, providing the limit horizontal acceleration associated to the longitudinal and transversal collapse as function of the bridge geometry. Several methodologies based on limit analysis have been also proposed to take into account the increased load carrying capacity of masonry road bridges, associated to strengthening interventions with fiber reinforced composites (D'Ambrisi *et al.* 2015, Bertolesi *et al.* 2018), or the effects related to settlements at springings (Di Carlo *et al.* 2018, Galassi *et al.* 2018, Zampieri *et al*. 2018).

Finite elements models have been also frequently used. Drosopoulos *et al.* (2006) proposed a method based on finite element analysis having interfaces with unilateral contact with friction. The method allows evaluating the collapse load using a path-following technique and considering the occurrence of cracking produced by the opening or sliding of some interfaces. Nonlinear analyses based on the FE method have been also performed by several authors, in order to assess the capacity of masonry bridges under seismic loads (Pelà *et al.* 2009, Pelà *et al.* 2013, Zampieri *et al.* 2015, Rovithis and Pitilakis 2016, Sayin 2016, Zampieri *et al.* 2017) or eccentric vertical loads, by investigating different 3D shapes (e.g., skew arches) and comparing the results with other codes based on limit analysis approach (Milani and Lourenço 2012).

The evaluation of masonry arch bridges by means of experimental investigations is definitely more complex and expensive and very few references can be found in the literature on real scale bridge tests (Page 1987, Brencich *et al.* 2016). Conversely, there exist several investigations carried out on reduced scale specimens of masonry arches with no fill (Huges *et al.* 1998, Krajewski and Hojdys 2015) or on very small scale models of arches with fill (Burroughs *et al.* 2002, Callaway *et al.* 2012).

As far as the seismic action is concerned, several studies exist for isolated masonry arches, both in static and dynamic field (Franciosi 1986, Oppenheim 1992, Clemente 1998, De Lorenzis *et al.* 2007, DeJong *et al.* 2008, Alexakis and Makris 2014, Calderini and Lagomarsino 2015, Cavalagli *et al.* 2016, Cavalagli *et al.* 2017, Severini *et al.* 2018, Stockdale *et al.* 2018), while other studies assume the presence of the backfill applying the seismic action to the external live load (Caporale *et al*. 2006). Within this context, the definition of a consistent model of the backfill effect on the masonry arch due to seismic load requires further investigations.

3. Description of the limit analysis based procedure

Let us consider a masonry arch bridge of circular shape with abutments. The problem considers the interaction between the structure and the surrounding backfill, typically constituted by granular material, under the action of the self-weight and the seismic loads.

The following parameters, shown in Fig. 1, define the geometry of the structure: span l, arch thickness s, rise f of the arch, height h and width g of the abutment, height h_c of the backfill at the crown. Moreover, a horizontal upper surface of the backfill and an out-of-plane depth d have been assumed.

3.1 Analytical development

The failure condition of a masonry arch bridge in presence of its self-weight, the weight of the backfill and the seismic action has been investigated by referring to the classical limit analysis procedure established by Heyman (1969). Thus, the following hypotheses have been assumed for the masonry: no-tensile strength, infinite compressive strength and no-sliding between the voussoirs. Three conditions are assumed to be verified at collapse: i) resistance criterion, ii) equilibrium and iii) mechanism condition. The first and second condition correspond to the existence of a line of thrust everywhere contained inside the boundary of the arch thickness and satisfying the equilibrium with the acting loads. In general, when seismic action is considered, the third condition requires the activation of a four-hinges mechanism. An iterative procedure, developed in MATLAB environment and briefly described below, has been used to determine the collapse mechanism and the corresponding seismic load multiplier.

The masonry arch bridge has been analyzed considering the presence of the circular arch, the abutments and the backfill, which has an horizontal overall dimension of l+2g, with the geometrical parameters introduced in the previous section. Since the backfill is taken into account uniquely as a load, the bearing structure is composed of the arch and the abutments. The analysis has been carried out as a 2D problem in the plane of the bridge. The arch and the

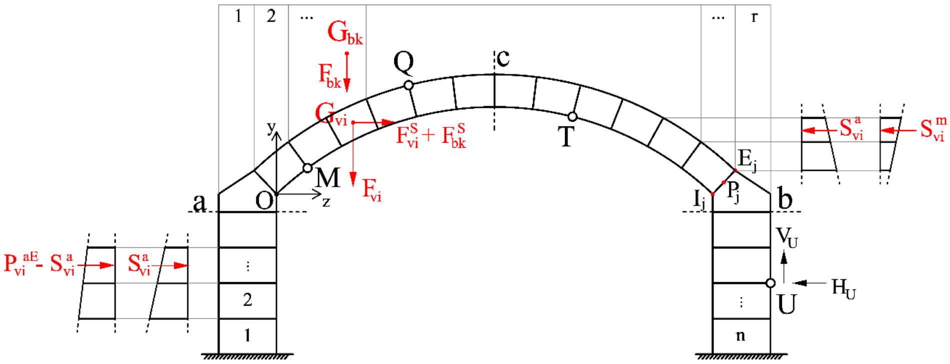

Fig. 2 Weight of voussoirs and backfill and inertial forces acting on the four-hinge arch

abutments are discretized into n voussoirs, numbered from left to right (Fig. 2). The resulting n+1 joints are obtained for the arch and the abutments by radial and horizontal cuts respectively. The four collapse hinges and the corresponding joints have been denoted by M, Q, T, U and by m, q, t, u.

After the definition of the geometrical parameters, the coordinates of the following points are determined by referring to the Cartesian reference system (z, y) of Fig. 2: center of gravity G_{vi} of the i^{th} voussoir, intrados I_j, extrados E_j and geometric center P_j of the j^{th} joint. The backfill is discretized into r elements obtained by intersecting the horizontal top line and the extrados with vertical lines starting from the points E_j, as shown in Fig. 2. The coordinates of the center of gravity G_{bk} of the k^{th} backfill element are then evaluated.

Still referring to Fig. 2, the structure is subjected to the action of the self-weight of the voussoirs F_{vi}, the backfill elements weight F_{bk}, the active S_a and mechanism S_m backfill pressure acting on the arch and abutments, the seismic increment of the active pressure P^{aE}-S^a and the seismic actions related to the mass of the voussoirs F^S_{vi} and backfill F^S_{bk}. The resultant loading system consists of vertical and horizontal loads applied at the centers of gravity of the voussoirs and backfill.

The self-weight of the i^{th} voussoir and of the k^{th} backfill element, applied at the corresponding centers of gravity G_{vi} and G_{bk}, can be evaluated as follows

$$F_{vi} = \gamma_v \cdot A_{vi} \cdot d \tag{1}$$

$$F_{bk} = \gamma_b \cdot A_{bk} \cdot d \tag{2}$$

where γ_v and γ_b represent the masonry and backfill specific weight respectively, A_{vi} the area of the i^{th} voussoir, A_{bk} the area of the k^{th} backfill element, with i=1 to n and k=1 to r. The seismic action is modelled through a system of horizontal forces proportional to the vertical weights of the voussoirs and the backfill through a multiplier μ; these forces are directed, without loss of generality, from left to right. The seismic force related to the i^{th} element of the arch or abutments is applied at the centre of gravity G_{vi}

$$F^S_{vi} = \mu \cdot F_{vi} \tag{3}$$

with i=1 to n. Based on the contents of the next paragraph, the seismic force associated with the mass of the backfill has been determined by considering only the masses placed on the left side of the bridge, thus resulting

$$F^S_{bk} = \mu \cdot F_{bk} \tag{4}$$

with k=1 to r/2, being each force applied at the center of gravity of the underneath voussoir (Fig. 2). This assumption relies on the fact that the seismic action on the backfill placed on the right side of the arch is mainly transmitted to the neighboring material by horizontal axial stresses, rather than transmitted by shear stresses to the underneath material.

3.1 Backfill horizontal pressure

In the evaluation of the seismic load multiplier μ, the pressure of the backfill on the arch and on the abutments cannot be neglected. Although in some papers the effect of the lateral active and passive pressure has been included (Ng and Fairfield 2004, Miriano *et al.* 2016), the role of the backfill in the in-plane seismic load bearing capacity of masonry arches still need to be further investigated.

The essential role played by the backfill in the stability of arched structures subjected to vertical loads is well known. It can be considered as composed by three different effects:

1) the stabilizing effect of the backfill self-weight;

2) the horizontal pressure produced by the backfill in static conditions on the lateral sides of the abutments;

3) the stabilizing effect of the backfill stiffness that produces a pressure distribution that opposes to the arch deformation.

Whereas the stabilizing effect of the backfill self-weight has been always considered in the assessment of masonry arches, only in the last decades the advantages arising from including its stiffness in the analysis have started to be taken into account. This effect is well documented, for instance, by Gago *et al.* (2011) who showed that loading distributions similar to that of the backfill self-weight in circular arches produce quasi circumferential lines of thrust. They also highlighted two favourable effects: the restriction of the lateral movement of the loaded voussoirs, giving rise to a smaller effective span of the arched structure, and the distribution over a wider length of the arch of any concentrated load applied to the top of the backfill. Molins and Roca (1998) were among the first to take into account the backfill stiffness, by means of its discretization into a

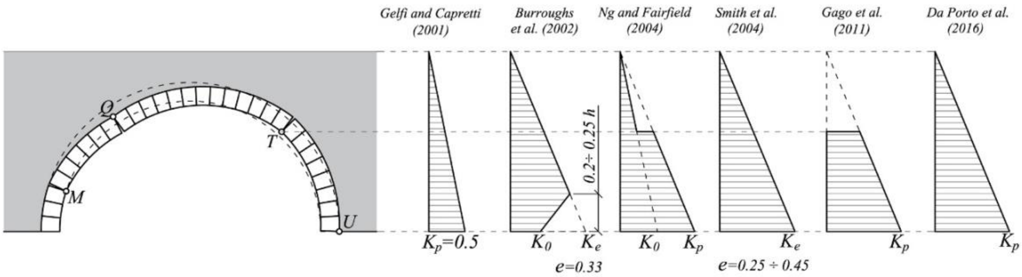

Fig. 3 Comparison of different passive pressure distributions used by different researchers

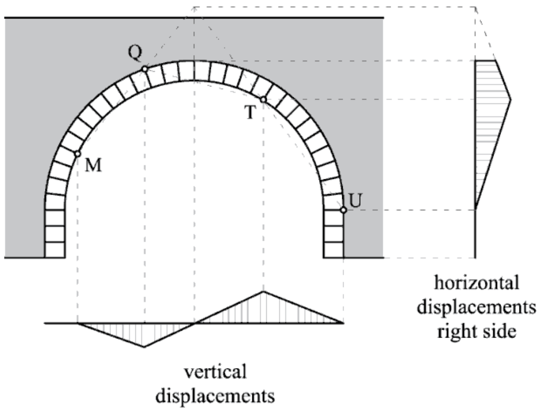

(a)

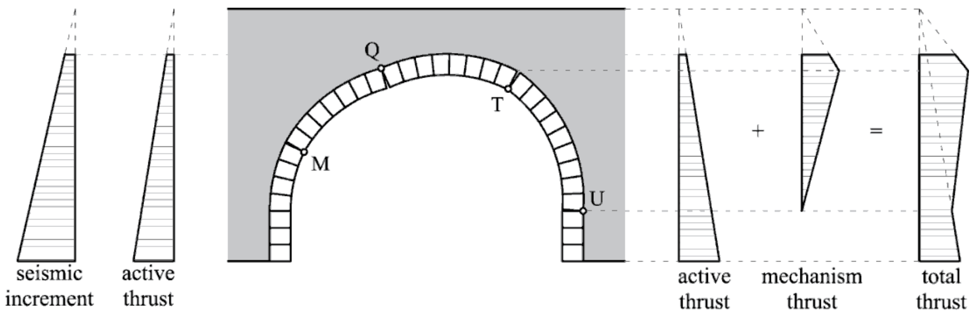

(b)

Fig. 4 (a) Kinematic mechanism and corresponding displacements of the masonry arch under vertical and horizontal loads. (b) Active pressures and mechanism thrust distributions at collapse used in LA method

system of equivalent linear elements. Their analysis showed that only when the active contribution of the spandrel infill was included, satisfactory agreement could be obtained between the numerical simulation and the corresponding experimental measurements. Recently, the effect of the backfill has been modelled by means of lateral springs (Callaway *et al.* 2012) or by means of horizontal pressures just behind the abutments. In this last case, the passive pressures have been derived from the general theories such as those stated by Rankine, Coulomb, Mononobe and Okabe. As well known, in these theories the equilibrium of a volume of soil that moves as a rigid body without internal deformations is analyzed taking into account the soil internal friction and the friction between the wall and the soil.

Nevertheless, very different assumptions on the value and the distribution of the passive pressures can be found in literature, as shown in Fig. 3. A constant value of the passive pressure coefficient K_p=0.5 has been proposed by Gelfi and Capretti (2001) in studying the stability of arches and vaults. Burroughs *et al.* (2002) proposed a modified lateral pressure coefficient K_e function of K_0 and K_p as

$$K_e = K_0 + e \cdot \left(K_p - K_0 \right) \tag{5}$$

in which e is an empirical parameter, calibrated through experimental tests, equal to 1/3.

Ng and Fairfield (2004) assumed a bi-linear backfill pressure distribution model, obtained using Rankine's theory with values of the coefficient of the horizontal pressure between the at rest value K_0 and the passive one K_P. Smith *et al.* (2004) adopted the model proposed by Burroughs *et al.* (2002) but with values for the coefficient e in the range 0.25÷0.45 and with a reduction in the lateral stress toward the hinge U as shown in Fig. 3. Gago *et al.* (2011) assumed the contribution of the backfill in the global equilibrium of the mechanism only between the two hinges T and U shown in Fig. 3. Da Porto *et al.* (2016) assumed a complete distribution of the active and of the passive pressures behind the abutments for the entire height of the backfill.

It can be observed that no agreement exists on the modelling of passive pressures in the analytical studies of the collapse mechanism of masonry arch bridges. Moreover, it seems that no one of the above mentioned analytical models can be generally adopted to describe the pressures generated by the effective collapse mechanism. This lack of agreement can be probably ascribed to the fact that the mentioned theories (Rankine, Coulomb, …) describe quite well the condition encountered in the case of retaining structures, but they cannot match the collapse mechanism occurring in the case of masonry arch bridges that differs significantly from a solid translation of a soil volume.

In the present work, the distribution and the entity of the passive pressure, called in the following "*mechanism thrust*", have been evaluated taking into account the shape of the mechanism at collapse. The idea, as shown in Fig. 4, is that the collapse mechanism produces a passive increment of horizontal pressure only in the volume of the backfill material interested by outwards displacements of the arch and abutments. It is assumed that the entity of the mechanism thrust is proportional to the horizontal deformation imposed to the backfill material by the horizontal displacement of the voussoirs at the collapse (Fig. 4(a)). This mechanism pressure distribution is then summed up to the active pressure distribution to obtain the total horizontal pressure distribution at collapse on the right side. The value of the maximum increment produced by the resistance of the backfill has been assumed equal to the value of the passive pressure calculated with the classical theories at the depth at which the maximum horizontal displacement is caused by the collapse mechanism.

Thus, a bi-linear distribution of the mechanism thrust has been applied to the portion of the arch that moves into the backfill, as shown in Fig. 4(b). Null values of pressure have been considered at the top backfill level and at the extreme right hinge U, while the maximum value of the passive pressure has been assumed in correspondence of the extrados point at joint t where hinge T takes place. The slope of the upper branch of the triangular diagram has been obtained from the Rankine passive pressure coefficient K_P

$$K_p = \frac{1+\sin\phi'}{1-\sin\phi'} \tag{6}$$

being ϕ' the friction angle of the backfill. Hence, the slope of both the upper and the lower branches of the diagram can be uniquely evaluated. This assumption agrees with the indications found in the literature (LimitState 2014) to take into account the improbable mobilization of the total passive pressure that would occur only in presence of high displacements of the structure. Hence, the total mechanism thrust is equal to

$$S^m = \frac{1}{2}\gamma_b K_p (f+s+h_c-y_{E_T})\cdot (f+s+h_c-y_U)\cdot d - \frac{1}{2}\gamma_b K_p h_c^2 \cdot d \tag{7}$$

being y_{E_T} the coordinate of the extrados point E_t of the joint corresponding to the hinge T and y_U the coordinate of the hinge U (Fig. 4(b)).

Finally, the active horizontal pressure of the backfill has been evaluated according to the Rankine theory, assuming planar failure surfaces and level backslope of the backfill. Hence, the active pressure coefficient is

$$K_a = \frac{1-\sin\phi'}{1+\sin\phi'} \tag{8}$$

and the total active thrust is equal to

$$S^a = \frac{1}{2}\gamma_b\ K_a\cdot(h+f+s+h_c)^2\cdot d - \frac{1}{2}\gamma_b K_a h_c^2\cdot d \tag{9}$$

It is clear that the proposed model for backfill pressures is approximated, since it ignores the stiffness and the resistance of the material placed at a level higher than that of the arch crown extrados, which opposes to the arch deformation.

According to (CEN 2008), masonry arch bridges subjected to in-plane seismic action can be considered as structures which essentially follow the horizontal seismic motion of the ground ("locked-in" structures). Thus, these structures do not experience significant amplification of the horizontal ground acceleration. Following the Mononobe-Okabe pseudo-static approach, the resultant active thrust in seismic condition P^{aE}, including the contribution of the static active pressure S^a, is equal to

$$P^{aE} = \frac{1}{2}\gamma_b\ K_{aE}\cdot(h+f+s+h_c)^2 (1-k_v)\cdot d - \frac{1}{2}\gamma_b K_{aE} h_c^2 (1-k_v)\cdot d \tag{10}$$

where K_{aE} is the Mononobe-Okabe active pressure coefficient

$$K_{aE} = \frac{\cos^2(\phi'-\theta-\psi)}{\cos\psi\cdot\cos^2\theta\cdot\cos(\delta+\theta+\psi)\left[1+\sqrt{\frac{\sin(\delta+\phi')\ \sin(\phi'-\beta-\psi)}{\cos(\delta+\theta+\psi)\ \cos(\beta-\theta)}}\right]^2} \tag{11}$$

$$\psi = \arctan\frac{k_h}{1-k_v} \tag{12}$$

The coefficient k_h is the horizontal ground acceleration due to the earthquake, while k_v=0.5 k_h is the vertical one. The parameter δ is the friction angle between the abutment and the backfill, θ is the inclination angle of the abutment surface respect to the vertical direction and β is the inclination angle of the top line of the backfill respect to the horizontal direction. The configuration of the adopted backfill pressures is shown in Fig. 4(b).

Moreover, it must be emphasized that the correct evaluation of the active and passive pressures is not a simple task for the impossibility of knowing, with the necessary accuracy, the geotechnical and mechanical properties of the backfill material, sometimes non-homogeneous, employed for the construction of masonry bridges.

3.3 Evaluation of the collapse condition

The collapse mechanism of the structure and the corresponding seismic load multiplier μ are attained by the following iterative procedure. A first trial configuration of the hinges position is assumed and the equilibrium imposed. If the resulting line of thrust, i.e., the line linking the centres of pressure of the normal force at each joint, is everywhere inside the arch thickness, the resistance criterion is satisfied and the solution is found. On the contrary, if the line of thrust falls outside the arch, the position of the hinges must be changed and the equilibrium imposed again. In order to get the right solution, each hinge is shifted toward the joint where the distance between the centre line of the arch and the line of thrust is maximum.

Let us denote by V_U and H_U the vertical and horizontal reactions at the hinge U (Fig. 2), by R_{vi} the resultant horizontal backfill pressure acting on the i^{th} voussoir and by $y_{R_{vi}}$ its application point coordinate, having assumed the resultant horizontal backfill pressure acting from left to right for the voussoirs with i=1 to n/2 and from right to left for the voussoirs with i=n/2+1 to n. Assuming that hinges M and Q take place at the left side of the structure, while T and U at the right one, the moment equilibrium about the hinges M, Q and T gives

$$
\begin{aligned}
&H_U(y_T - y_U) + V_U(z_T - z_U) - \sum_{i=1}^{n_{tu}} F_{vi}(z_T - z_{G_{vi}}) - \sum_{k=1}^{r_{\omega\xi}} F_{bk}\left(z_T - z_{G_{bk}}\right) \\
&\qquad + \sum_{i=1}^{n_{tu}} R_{vi}(y_T - y_{R_{vi}}) - \mu \cdot \sum_{i=1}^{n_{tu}} F_{vi}(y_T - y_{G_{vi}}) = 0 \\
&H_U(y_Q - y_U) + V_U(z_Q - z_U) - \sum_{i=1}^{n_{qu}} F_{vi}(z_Q - z_{G_{vi}}) - \sum_{k=1}^{r_{\eta\xi}} F_{bk}\left(z_Q - z_{G_{bk}}\right) \\
&\quad - \sum_{i=1}^{n_{qc}} R_{vi}(y_Q - y_{R_{vi}}) + \sum_{i=1}^{n_{cu}} R_{vi}(y_Q - y_{R_{vi}}) - \mu \cdot \sum_{i=1}^{n_{qu}} F_{vi}(y_Q - y_{G_{vi}}) \\
&\qquad - \mu \cdot \sum_{k=1}^{r_{\eta c}} F_{bk}(y_Q - y_{G_{vk}}) = 0 \\
&H_U(y_M - y_U) + V_U(z_M - z_U) - \sum_{i=1}^{n_{mu}} F_{vi}(z_M - z_{G_{vi}}) - \sum_{k=1}^{r_{\zeta\xi}} F_{bk}\left(z_M - z_{G_{bk}}\right) + \\
&\quad - \sum_{i=1}^{n_{mc}} R_{vi}(y_M - y_{R_{vi}}) + \sum_{i=1}^{n_{cu}} R_{vi}(y_M - y_{R_{vi}}) - \mu \cdot \sum_{i=1}^{n_{mu}} F_{vi}(y_M - y_{G_{vi}}) \\
&\qquad - \mu \cdot \sum_{k=1}^{r_{\zeta c}} F_{bk}(y_M - y_{G_{vk}}) = 0
\end{aligned}
\tag{13}
$$

where n and r refer respectively to the number of voussoirs and the backfill elements, with the associated subscripts that identify the delimiting joints. In detail: n_{tu}, n_{qu} and n_{mu} represent respectively the number of voussoirs between the joints t-u, q-u and m-u; n_{qc} (n_{mc}) is the number of voussoirs between the joint q (m) and the joint at the crown c= n/2+1, while n_{cu} is the number of voussoirs between the joint at the crown c and u. Relatively to the backfill: $r_{\omega\xi}$, $r_{\eta\xi}$ and $r_{\zeta\xi}$ represent respectively the number of backfill elements placed above the voussoirs included between the joints ω, η, ζ and ξ; $r_{\eta c}$ and $r_{\zeta c}$ represent respectively the number of backfill elements placed above the voussoirs included between the joints η, ζ and c, being: ω=t or b if the hinge T is placed respectively on the arch or on the right abutment, ξ=u or b if the hinge U is placed respectively on the arch or on the right abutment, η=q or a if the hinge Q is placed respectively on the arch or on the left abutment, ζ=m or a if the hinge M is placed respectively on the arch or on the left abutment (Fig. 2). The system of equations (13) can be solved in order to provide the reactions at hinge U and the seismic load multiplier μ. The complete knowing of the loading system allows the determination of the eccentricity of the normal force at each joint and the drawing of the line of thrust. In order to verify if the line of thrust, obtained by linking the centres of pressure, is anywhere inside the masonry, the following conditions must be satisfied at each joint of the arch and abutment respectively

$$-\frac{s}{2} \le e_j \le \frac{s}{2} \tag{14}$$

$$-\frac{g}{2} \le e_j \le \frac{g}{2} \tag{15}$$

for j=1 to n+1. It should be noticed that the sign of equality holds only in correspondence of the joints m, q, t and u. If the resistance criterion is satisfied, then the position of hinges identifies the actual failure mechanism and the corresponding seismic load multiplier. Otherwise, necessarily the hinges have to be moved and the procedure repeated. Further details about the iterative procedure can be found in (Cavalagli *et al.* 2016).

As an example, in Fig. 5 is reported the application of the proposed analytical procedure to the case of a masonry arch having the following geometrical properties: l=10.0 m, s=0.8 m, f=4.0 m, h=3.0 m, g=1.4 m, h_c=1.0 m, and d=1.0 m. The yellow line inside the arch represents the thrust line at the collapse, which is tangent to the four hinges highlighted with green circles. On the left and on the right of the bridge scheme, the pressure diagrams related to the backfill effect are plotted. In particular, the red diagrams indicate the active pressure distributions, the green diagram represents the seismic increment contribution and the magenta distribution describes the mechanism thrust related to the four-hinges mechanism. The blue diagrams show the total pressure distributions on the left and right side of the bridge. In all the analyses the structures have been

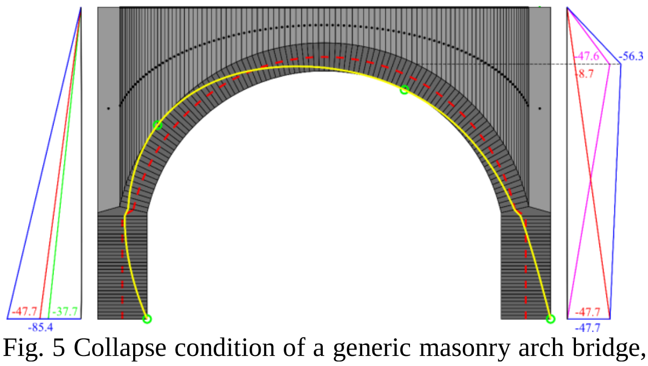

Fig. 5 Collapse condition of a generic masonry arch bridge, having f/l=0.4, with active pressure diagrams (red lines), seismic pressure increment (green line), distribution of the mechanism thrust (magenta line) and total pressure distributions (blue lines) on the left and right sides (stress values expressed in kN/m^2)

Table 1 Mechanical and geotechnical parameters assumed in the LA method

γ_v [kN/m^3]	γ_b [kN/m^3]	ϕ' [deg]	θ [deg]	δ [deg]	β [deg]
20	20	35	0	0	0

Table 2 Geometrical parameters of the four bridges analyzed (lengths expressed in m).

Case	f/l	l	s	f	h	g	h_c	d
1	0.2	10.0	0.8	2.0	3.0	1.4	1.0	1.0
2	0.3	10.0	0.8	3.0	3.0	1.4	1.0	1.0
3	0.4	10.0	0.8	4.0	3.0	1.4	1.0	1.0
4	0.5	10.0	0.8	5.0	3.0	1.4	1.0	1.0

discretized in a sufficient number of vossuoirs (n=100) in order to obtain results as much as possible closed to a continuous solution. This aspect has been just clarified in a previous work; the interested reader is invited to see (Cavalagli *et al.* 2016). In Table 1 the structure and backfill parameters used in the analysis are summarized.

4. Performance of the proposed limit analysis procedure

In order to evaluate the effectiveness of the proposed LA procedure, a Finite Element (FE) numerical model has been developed, by referring to the geometrical parameters introduced in Section 3 for the bridge description, and including a significant portion of the surrounding soil to study the pressure effects acting on the structure (Fig. 6(a)).

A parametric investigation has been performed considering different values of the arch rise/span ratio to analyze the role of the arch shape, from shallow to round arches, on the structure seismic capacity and to evaluate the performance of the LA method comparing the results with those obtained by the FE method. The following ratios of f/l have been assumed: 0.2, 0.3, 0.4 and 0.5. It should be noted that the values of rise and span are referred to the intrados profile of the bridge (see Fig. 1). The geometrical parameters of the investigated arch bridges are summarized in Table 2.

4.1 Finite element modelling

The numerical model, made up of four- and three-node elements with reduced integration, has been implemented with the commercial code ABAQUS v6.14 (2014). More in detail, a structured mesh has been adopted in the arch and in the lower soil layer, while a free mesh type has been used in the backfill (Fig. 6(b)). In order to better represent the horizontal pressure, a large portion of the soil around the bridge has been considered. Non-linear analyses have been performed in plane strain condition.

Particular attention has been devoted to the boundary conditions in order to represent a consistent response of the structural model. A soil layer has been included at the base of the arch to avoid stress concentrations related to the direct application of the restraint conditions to the backfill and to the abutments. Moreover, in order to obtain a better distribution of the vertical loads under the abutments, an expansion of the bridge footprint with the same mechanical properties of masonry has been introduced, to simulate the presence of a foundation. In the lateral right side of the model, only the horizontal displacements have been prevented. In the left side, a rigid bound has been included with a unilateral contact between the two surfaces, in order

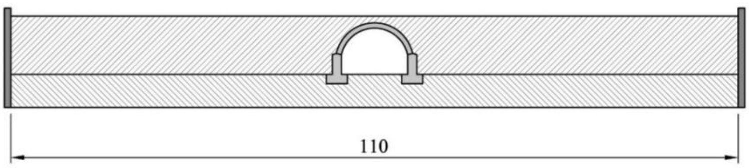

(a)

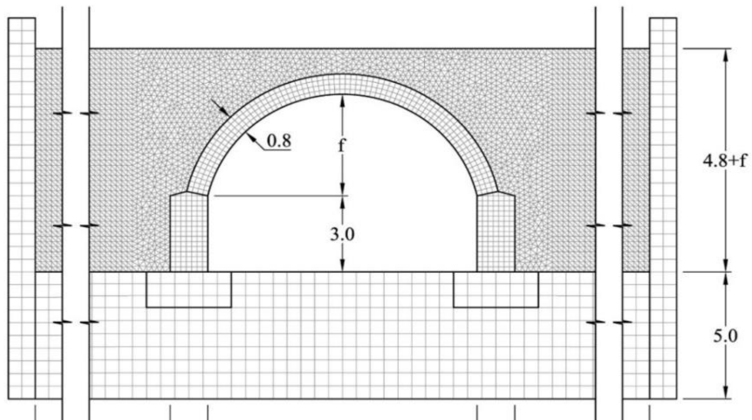

(b)

Fig. 6 FE model of the investigated masonry arches with f =2.0, 3.0, 4.0 and 5.0 m. (lengths expressed in m)

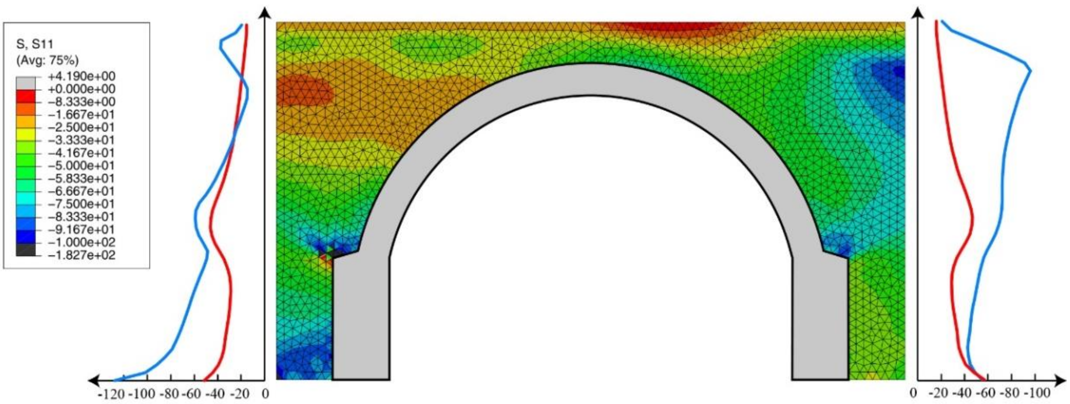

Fig. 7 Colour map of the horizontal pressure distribution developed into the backfill and horizontal pressures on two vertical sections placed 1.4 m behind the abutments after the application of gravitational (red lines) and the seismic (blu) loads (stress values expressed in kN/m^2)

Table 3 Mechanical and geotechnical parameters used in the FE method

Material	Property	*u.m.*	value
Masonry	Mass density	kg/m^3	2e+0.3
	Elastic modulus	kN/m^2	1.5e+07
	Poisson's ratio	-	0.2
	Compression strength	kN/m^2	4500
	Tensile strength	kN/m^2	150
Backfill	Mass density	kg/m^3	2e+0.3
	Elastic modulus	kN/m^2	3e+05
	Poisson's ratio	-	0.2
	Friction angle	deg	35
	Dilation angle	deg	20
	Cohesion	kN/m^2	2

to allow their separation in presence of the seismic loads acting from left to right. The contact condition between the backfill and the structural arch has been modelled with a classical node-to-surface formulation. In this case, the application of a friction coefficient in the unilateral contact law allowed describing the pressure effects on the abutments and the arch in a more consistent way.

An isotropic behaviour has been considered for the materials in the elastic range, while the classical Mohr-Coulomb criterion and the Concrete Damaged Plasticity model have been used for the description of the backfill and the masonry respectively beyond the elastic limit. Regarding the first, a good agreement exists in the literature on the assumption adopted for the backfill modelling in numerical analyses carried out by FE methods. In fact, the Mohr-Coulomb criterion has been used in almost all investigations for both cohesive (Cavicchi and Gambarotta 2005, Drosopoulos *et al.* 2006) and cohesionless (Gago *et al.* 2001) soils. Concerning the latter, the Concrete Damaged Plasticity model is suitable to describe the nonlinear behaviour, both in tension and compression, and the possible damage development in masonry materials (Cavalagli and Gusella 2015, Tiberti *et al.* 2016, Bertolesi *et al.* 2017). Tension stiffening with softening behaviour has been considered, taking from the literature the data for the path description of both the post-peak phases. The mechanical and geotechnical parameters used in the FE analyses are summarised in Table 3.

The gravitational and the seismic loads have been applied in two different steps to investigate the related effects of the backfill in terms of horizontal pressures on the structure. In the first step the gravitational acceleration has been applied, while in the latter a linear increasing horizontal acceleration has been introduced. Force-controlled numerical analyses have been performed up to the achievement of the convergence limit.

As an example, in Fig. 7 the results obtained for the case with f/l=0.4 are shown in terms of the horizontal stress distribution developed inside the backfill. At the sides of the image, the diagrams of the horizontal pressures behind the abutments have been reported at a distance equal to the abutments thickness (1.4 m), in order to avoid the local stress concentrations at the arch springing due to the geometrical changes. The red graphs are related to the application of the gravitational loads, while the blue ones describe the total horizontal pressure produced by the application of the gravitational and seismic loads.

4.2 Analysis of results

Several comments can be deduced looking at the results of the parametric investigations. First of all, it can be observed that the hypothesis on the shape of the pressure distribution shown in Fig. 4(b) is confirmed by the data shown in the graph of Fig. 7. In fact, it can be observed that, neglecting the perturbation of the horizontal pressures in correspondence of the transition zone between the abutment and the arch vault, the total pressure distribution at the vertical section on the right of the arch describes a bi-linear relation with maximum values approximately in correspondence of the 3rd hinge of the arch mechanism. Further evidence of this behaviour can be obtained looking at the graphs of Fig. 8, where the increment of the horizontal pressure produced by the seismic action is plotted for the four investigated cases. In particular the grey dashed lines represent the increment of horizontal pressures, after the application of the gravitational load, obtained in

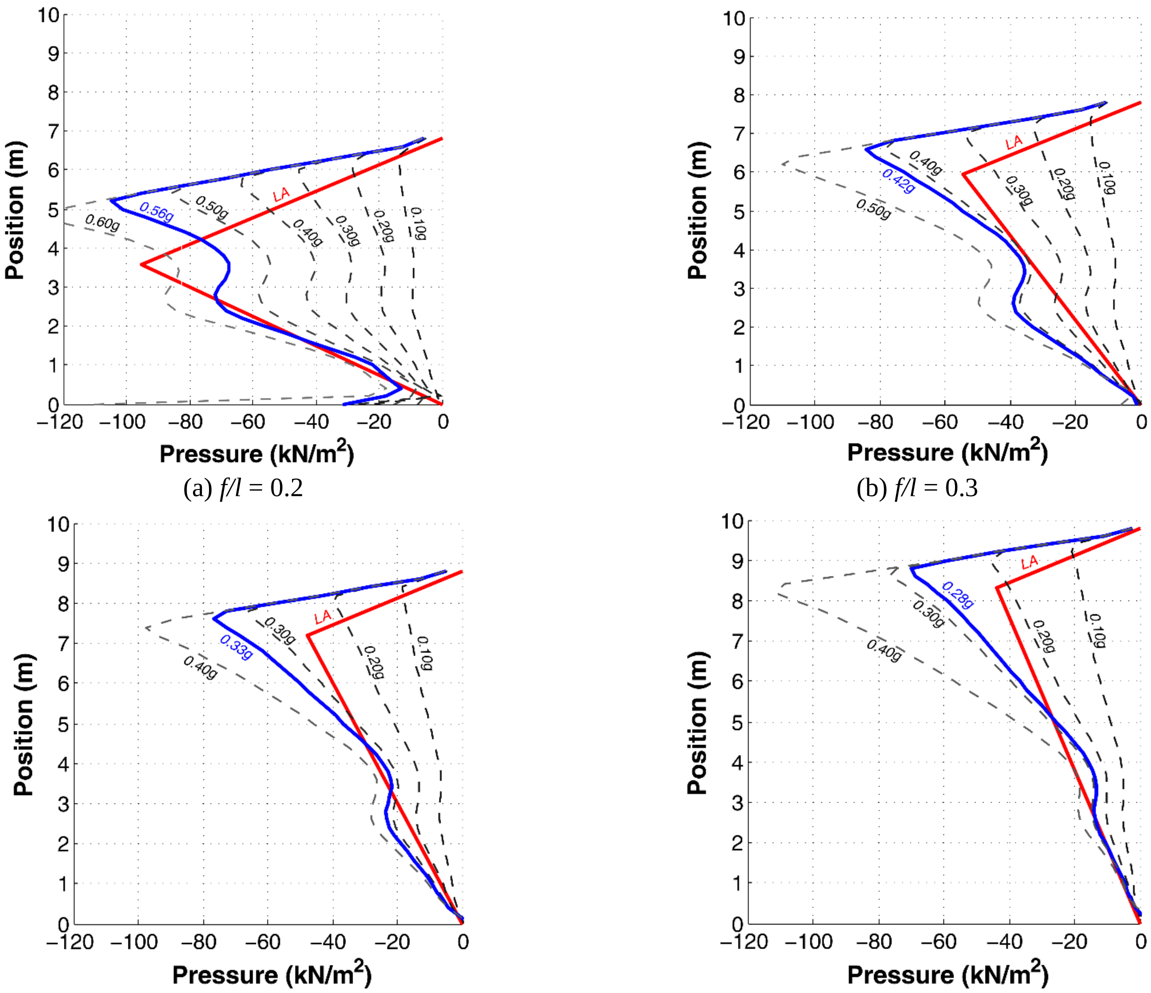

(a) *f/l* = 0.2 (b) *f/l* = 0.3

(c) *f/l* = 0.4 (d) *f/l* = 0.5

Fig. 8 Comparison between the increments of the horizontal pressures under seismic action on the vertical section behind the right abutment resulting from the FE model (blue and dashed grey curves) and those assumed in LA method (red curves) for the different investigated cases. The blue curves have been obtained in correspondence of acceleration values equal to the load multipliers provided by the LA procedure

the FE model, at a distance of 1.4 m from the right abutment, for increasing values of the seismic acceleration. The generic blue line corresponds to the mechanism pressures at a value of acceleration equal to the load multiplier μ evaluated by the LA procedure; the mechanism thrust obtained by limit analysis is represented in red color. A good agreement can also be observed in terms of distribution shape for the left diagrams of Fig. 7 which result very similar to those of the active pressure and of the seismic pressure increment used in LA method, shown in Fig. 4(b). Some observations can be done also for the maximum value of the mobilized mechanism thrust. This value depends on the depth below the upper surface of the backfill at which the maximum occurs, on the bridge displacements caused by the seismic action and on the capacity of the arch itself to sustain horizontal displacements before the formation of the four- hinges mechanism. Again from Fig. 8 it can be observed that the maximum value of the horizontal pressure assumed in the LA investigations (continuous red line) is quite close to that obtained with the FE method (continuous blue line) in correspondence of the same value of the seismic acceleration, both in terms of intensity and position. Moreover, it can be noticed that LA method gives conservative (smaller) values of the mechanism pressures for all the analyzed cases.

Regarding the results obtained through the FE model, the detection of the instant that can be assumed as that corresponding to the formation of the four-hinge mechanism is not straightforward. In the present work it has been evaluated from the equilibrium path of a reference point (mid thickness of the keystone), which describes the horizontal displacement versus the applied seismic load intensity. These graphs for the four investigated cases are shown in Fig. 9. As expected, a relevant change in the stiffness of the masonry arch occurs as consequence of the progressive diffusion of plastic deformation.

Nevertheless, in the FE model the formation of this mechanism does not occur instantaneously but it builds up for increasing values of the external seismic load. In this situation the value of the seismic intensity that produces the formation of the collapse mechanism has been evaluated

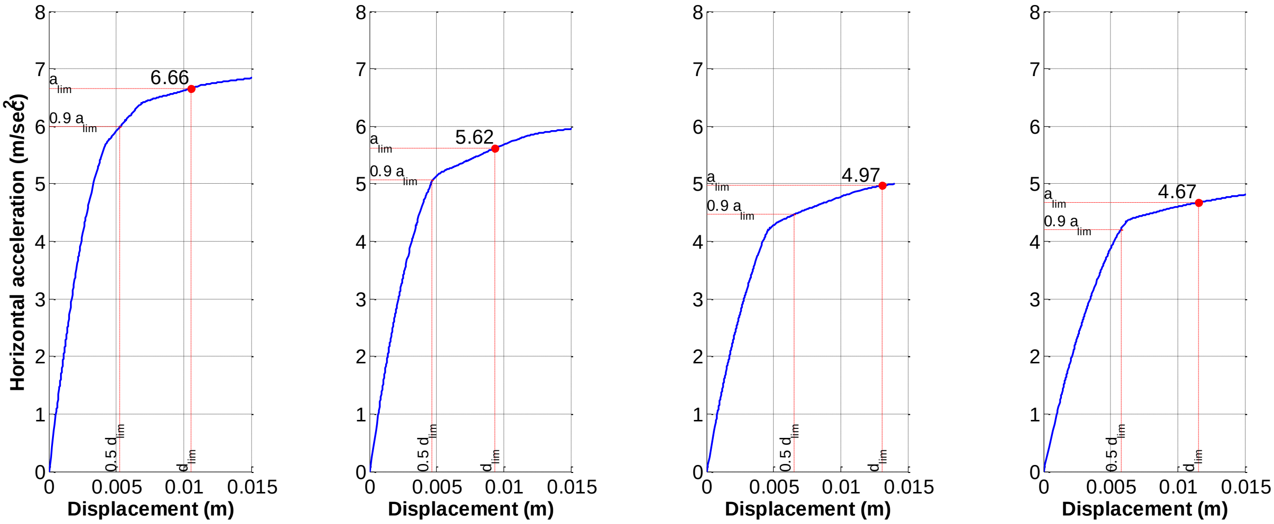

(a) f/l=0.2 (b) f/l=0.3 (c) f/l=0.4 (d) f/l=0.5

Fig. 9 Equilibrium path of the reference point (blue curves) and collapse conditions (red dots) for the different investigated cases

Table 4 Comparison between the collapse conditions obtained by LA and FE models in terms of horizontal accelerations

Case	Seismic acceleration at collapse (m/s^2)		
	LA	FE	Difference (%)
1	5.48	6.66	-17.7
2	4.12	5.62	-26.7
3	3.28	4.97	-34.0
4	2.76	4.67	-40.9

with a procedure used in geotechnical engineering (Brinch-Hansen 1963). The ultimate value of the horizontal acceleration a_{lim} is the value associated with twice the displacement of the reference point as obtained for 90% of a_{lim} itself. Applying this procedure to the non-linear curves obtained by plotting the horizontal displacement of the reference point vs the intensity of the seismic action (Fig. 9), the values of the seismic action that causes the collapse listed in Table 4 have been obtained. In the same table are listed also the corresponding values of the seismic action obtained with the LA method and the difference values in percentage related to each case. It should be noted that the results obtained by the proposed procedure are more conservative with respect to the results given by FE models, since a significant level of safety is required for these types of analysis. In particular, such a result highlights as this method is suitable for large scale applications allowing the rapid identification of the most critical situations when several structures are analyzed.

The comparison of the collapse mechanisms obtained with the two methods is carried out in Figs. 10 and 11. The color maps in Fig. 10 represent the intensities of the plastic deformations obtained with the FE method, which are localized in the arch sections corresponding to the plastic hinges. In the same graphs, the red curves represent the lines of thrust obtained with the LA method. The red dots indicate the points where the line of thrust is tangent to the

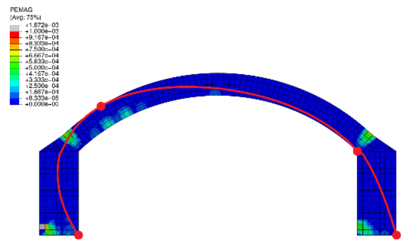

(a) f/l = 0.2

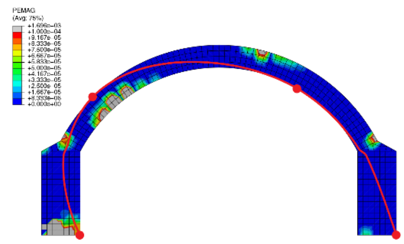

(b) f/l = 0.3

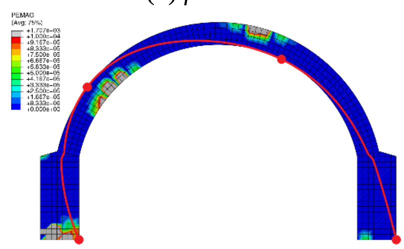

(c) f/l = 0.4

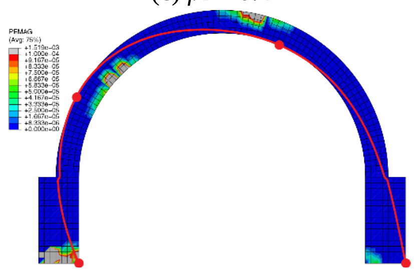

(d) f/l = 0.5

Fig. 10 Comparison between plastic strains (FE) and line of thrust (LA) for the different investigated cases

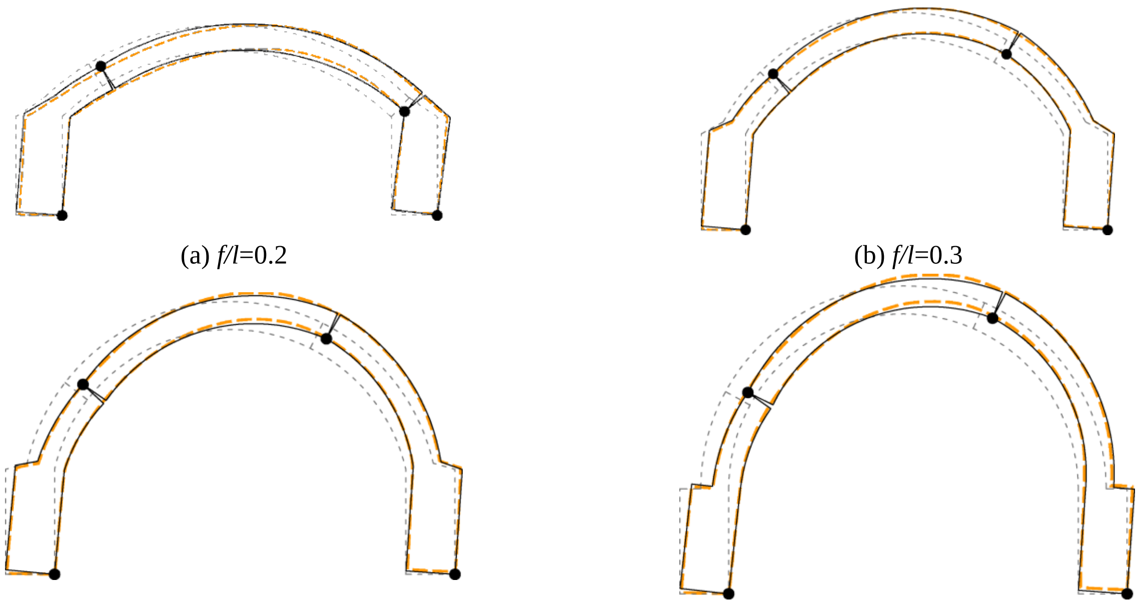

(a) *f*/*l*=0.2 (b) *f*/*l*=0.3

(c) *f*/*l*=0.4 (d) *f*/*l*=0.5

Fig. 11 Comparison between deformed configuration of the FE model (dashed orange profile) and collapse mechanism obtained by limit analysis (continuous black profile), superimposed to the initial configuration (dashed grey profile)

arch cross section and represent the hinges positions. It can be observed a general good agreement between the results of the two methods, especially in consideration of the spread damaged zones given by the FE models due to the evolution of the mechanisms during the analyses. Moreover, it must be considered that the damaged zones observed at the springings of the arch for the two bridges with *f*/*l*=0.2 and *f*/*l*=0.3 are related to the application of the gravitational loads, so that they cannot be ascribed to the horizontal actions, except for the right hinge of the case *f*/*l*=0.2.

In Fig. 11 the shapes of the deformed configurations obtained by LA and FE models are superimposed to compare the collapse mechanisms given by the two methods. It should be noted that, in the case of LA model, only the position of the hinges is defined. The kinematic configuration has been determined by fixing the rigid rotation of the first left rigid body over the deformed shape of the FE model; then the remaining parts of the structure follow the kinematic chain corresponding to the collapse mechanism configuration. The figure shows a good agreement between the results obtained with LA and FE models, highlighting the effectiveness of the proposed model also in terms of collapse mechanisms.

5. Conclusions

In this paper the problem of the in-plane seismic capacity of masonry arch bridges has been studied. A procedure, based on limit analysis, has been developed in order to achieve a rapid estimation of the horizontal collapse condition. The classical Heyman's assumptions on masonry, no-tensile strength, infinite compressive strength and pure rotational failure at collapse, have been assumed. The solution has been reached by searching the limit equilibrium condition of the structure through an iterative algorithm. Attention has been dedicated to the description of the inertial effect of the backfill and to the evaluation of the lateral backfill pressures.

The active thrust, evaluated following Rankine theory, has been considered to act on the arch and abutments, while the seismic increment of active thrust has been taken into account by referring to the Mononobe-Okabe approach. Regarding the pressures provided by the backfill resistance, a novel modelling of the backfill effect has been proposed, which considers the structural kinematic configuration at collapse for the definition of the so called *mechanism thrust*.

In order to evaluate the performance of the proposed LA procedure, finite element (FE) models have been carried out and the results, obtained by the two methods on four masonry arch bridges with different values of rise/span ratio, have been compared.

The comparisons have been made in terms of kinematic mechanism, collapse multiplier and horizontal pressures induced by the backfill on the structure. The kinematic mechanisms obtained at the collapse by both methods, LA and FE, are in a good agreement, i.e., the positions of the hinges in the LA mechanisms fall into the plastic zones of the FE models. Concerning the collapse multiplier, the LA method seems to be more conservative than the other one, even if it has to be noted that the ultimate conditions considered in the FE method are related to horizontal accelerations at which the plastic deformations have been already developed in the structure. The differences between the two models increase for higher values of the ratio *f*/*l*. Regarding the horizontal pressure distributions of the backfill on the bridge structure, the comparison highlights a good agreement between the two methods, especially for the active pressure and the increment of the seismic load. The new model proposed for the passive pressure distribution well reproduces the pressure diagrams obtained in the FE models showing, at the same time, some differences on their peak values, corresponding to the same horizontal accelerations.

Certainly, the LA method provides fast but approximated (conservative) evaluations and, therefore, is more suitable to be used for large scale analysis, e.g., those carried out to manage specific road or railways networks when the availability of limited budgets requires the definition of a prioritization list of interventions. The FE method can give more accurate information regarding the structural response of a specific case study, introducing material properties in a more consistent way, but it requires very skilled engineers to build up reliable FE models.

References

ABAQUS V6.14 (2014), Analysis User's Guide, Dessault Systèmes Simulia Corp., Providence, RI, USA.

Alexakis, H. and Makris, N. (2014), "Limit equilibrium analysis and the minimum thickness of circular masonry arches to withstand lateral inertial loading", *Arch. Appl. Mech.*, **84**, 757-772.

Bertolesi, E., Milani, G., Carozzi, F.G. and Poggi, C. (2018), "Ancient masonry arches and vaults strengthened with TRM and FRP composites: numerical analyses", *Compos. Struct.*, **187**, 385-402.

Bertolesi, E., Milani, G., Lopane, F.D. and Acito, M. (2017), "Augustus Bridge in Narni (Italy): Seismic vulnerability assessment of the still standing part, possible causes of collapse, and importance of the roman concrete infill in the seismic-resistant behavior", *Int. J. Arch. Heritage*, **11**(5), 717-746.

Brencich, A., Cassini, G. and Pera, D. (2016), "Load bearing structure of masonry bridges", *Proceedings of the 8th International Conference on Arch Bridges*, Wroklaw, Poland, October.

Brinch-Hansen, J. (1963), "Hyperbolic stress-strain response: Cohesive soils", Discussion, *Am. Soc. Civil Eng. J. Soil Mech. Found. Div.*, **89**(SM4), 241-242.

Burroughs, P., Hughes, T.G., Hee, S. and Davies, M.C.R. (2002), "Passive pressure development in masonry arch bridges", *Proc. Inst. Civil Eng. Struct. Build.*, **153**, 331-339.

Calderini, C. and Lagomarsino, S. (2015), "Seismic response of masonry arches reinforced by tie-rods: Static tests on a scale model", *J. Struct. Eng.*, **141**(5), 4014137.

Callaway, P., Gilbert, M. and Smith, C.C. (2012), "Influence of backfill on the capacity of masonry arch bridges", *Proc. Inst. Civil Eng.: Bridge Eng.*, **165**(3), 147-158.

Caporale, A., Luciano, R. and Rosati, L. (2006), "Limit analysis of masonry arches with externally bonded FRP reinforcements", *Comput. Meth. Appl. Mech. Eng.*, **196**(1-3), 247-260.

Cavalagli, N. and Gusella, V. (2015), "Dome of the Basilica of Santa Maria degli Angeli in Assisi: Static and dynamic assessment", *Int. J. Arch. Heritage*, **9**(2), 157-175.

Cavalagli, N., Gusella, V. and Severini, L. (2016), "Lateral loads carrying capacity and minimum thickness of circular and pointed masonry arches", *Int. J. Mech. Sci.*, **115-116**, 645-656.

Cavalagli, N., Gusella, V. and Severini, L. (2017), "The safety of masonry arches with uncertain geometry", *Comput. Struct.*, **188**, 17-31.

Cavicchi, A. and Gambarotta, L. (2005), "Collapse analysis of masonry bridges taking into account arch-fill interaction", *Eng. Struct.*, **27**, 605-615.

CEN-European Committee for Standardization (2008), EN 1998-2 Eurocode 8-Design of Structures for Earthquake Resistance Part 2: Bridges, Brussels (B).

Clemente, P. (1998), "Introduction to dynamics of stone arches", *Earthq. Eng. Struct. Dyn.*, **27**, 513-522.

D'Ambrisi, A., Focacci, F., Luciano, R., Alecci, V. and De Stefano, M. (2015), "Carbon-FRCM materials for structural upgrade of masonry arch road bridges", *Compos. Part B*, **75**, 355-366.

Da Porto, F., Tecchio, G., Zampieri, P., Modena, C. and Prota, A. (2016), "Simplified seismic assessment of railway masonry arch bridges by limit analysis", *Struct. Infrastr. Eng.*, **12**, 567-591.

De Lorenzis, L., DeJong, M. and Ochsendorf, J. (2007), "Failure of masonry arches under impulse base motion", *Earthq. Eng. Struct. Dyn.*, **36**, 2119-2136.

De Santis, S. and De Felice, G. (2014), "A fibre beam-based approach for the evaluation of the seismic capacity of masonry arches", *Earthq. Eng. Struct. Dyn.*, **43**, 1661-1681.

DeJong, M., De Lorenzis, L., Adams, S. and Ochsendorf, J. (2008), "Rocking stability of masonry arches in seismic regions", *Earthq. Spectra*, **24**(4), 847-865.

Di Carlo, F., Coccia, S. and Rinaldi, Z. (2018), "Collapse load of a masonry arch after actual displacements of the supports", *Arch. Appl. Mech.*, **88**(9), 1545-1558.

Drosopoulos, G.A., Stavroulakis, G.E. and Massalas, C.V. (2006), "Limit analysis of a single span masonry bridge with unilateral frictional contact interfaces", *Eng. Struct.*, **28**, 1864-1873.

Franciosi, C. (1986), "Limit behaviour of masonry arches in the presence of finite displacements", *Int. J. Mech. Sci.*, **28**(7), 463-471.

Gago, A.S., Alfaiate, J. and Lamas, A. (2011), "The effect of the infill in arched structures: Analytical and numerical modelling", *Eng. Struct.*, **33**(5), 1450-1458.

Galassi, S., Misseri, G., Rovero, L. and Tempesta, G. (2018), "Failure modes prediction of masonry voussoir arches on moving supports", *Eng. Struct.*, **173**, 706-717.

Gelfi, P. and Capretti, A. (2001), "Backfill role on the stability of arches and vaults", *Tran. Built Environ.*, **55**, 295-304.

Gioffré, M., Gusella, V. and Cluni, F. (2008), "Performance evaluation of monumental bridges: Testing and monitoring 'Ponte delle Torri' in Spoleto", *Struct. Infrastr. Eng.*, **4**(2), 95-106.

Heyman, J. (1969), "The safety of masonry arches", *Int. J. Mech. Sci.*, **11**, 363-385.

Huges, T.G., Davies, M.C.R. and Taunton, P.R. (1998), "The influence of soil and masonry type on the strength of masonry arch bridges", *Arch Bridges. History, Analysis, Assessment, Maintenance and Repair*, Ed. A. Sinopoli, *Proceeding of the Second International Arch Bridge Conference*, Venice, Italy, October.

Krajewski, P. and Hojdys, Ł. (2015), "Experimental studies on buried barrel vaults", *Int. J. Arch. Heritage*, **9**, 834-843.

LimitState: RING Manual (2014), Version 3.1.a., LimitState Ltd, Sheffield, United Kingdom.

Milani, G. and Lourenço P.B. (2012), "3D non-linear behavior of masonry arch bridges", *Comput. Struct.*, **110-111**, 133-150.

Miriano, C., Cattoni, E. and Tamagnini, C. (2016), "Advanced numerical modelling of seismic response of a propped RC diaphragm wall", *Acta Geotechnica*, **11**, 161-175.

Molins, C. and Roca, P. (1998), "Capacity of masonry arches and spatial frames", *J. Struct. Eng.*, **124**(6), 653-663.

Ng, K.H. and Fairfield, C.A. (2004), "Modifying the mechanism method of masonry arch bridge analysis", *Constr. Build. Mater.*, **18**(2), 91-97.

Oppenheim, I. (1992), "The masonry arch as a four-link mechanism under base motion", *Earthq. Eng. Struct. Dyn.*, **21**, 1005-1017.

Page, J. (1987), "Load tests to collapse on two arch bridges at

Preston, Shropshire and Prestwood, Staffordshire”, Department of Transport, TRRL Research report 110, Crowthorne, England.
Pelà, L., Aprile, A. and Benedetti, A. (2009), “Seismic assessment of masonry arch bridges”, *Eng. Struct.*, **31**(8), 1777-1788.
Pelà, L., Aprile, A. and Benedetti, A. (2013), “Comparison of seismic assessment procedures for masonry arch bridges”, *Constr. Build. Mater.*, **38**, 381-394.
Rovithis, E.N. and Pitilakis, K.D. (2016), “Seismic assessment and retrofitting measures of a historic stone masonry bridge”, *Eartq. Struct.*, **10**(3), 645-667.
Sarhosis, V., De Santis, S. and De Felice, G. (2016), “A review of experimental investigations and assessment methods for masonry arch bridges”, *Struct. Infrastr. Eng.*, **12**(11), 1439-1464.
Sayin, E. (2016), “Nonlinear seismic response of a masonry arch bridge”, *Eartq. Struct.*, **10**(2), 483-494.
Severini, L., Cavalagli, N., DeJong, M. and Gusella, V. (2018), “Dynamic response of masonry arch with geometrical irregularities subjected to a pulse-type ground motion”, *Nonlin. Dyn.*, **91**(1), 609-624.
Smith, C.C., Gilbert, M. and Callaway, P.A. (2004), “Geotechnical issues in the analysis of masonry arch bridges”, *Proceedings of the 4th International Conference on Arch Bridges*, **3**, Barcelona, Spain, November.
Stockdale, G., Tiberti, S., Camilletti, D., Sferrazza Papa, G., Basshofi Habieb, A., Bertolesi, E., Milani, G. and Casolo, S. (2018), “Kinematic collapse load calculator: Circular arches”, *Software X*, **7**, 174-179.
Tiberti, S., Acito, M. and Milani, G. (2016), “Comprehensive FE numerical insight into Finale Emilia Castle behavior under 2012 Emilia Romagna seismic sequence: Damage causes and seismic vulnerability mitigation hypothesis”, *Eng. Struct.*, **117**, 397-421.
Zampieri, P., Cavalagli, N., Gusella, V. and Pellegrino, C. (2018), “Collapse displacements of masonry arch with geometrical uncertainties on spreading supports”, *Comput. Struct.*, **208**, 118-129.
Zampieri, P., Zanini, M.A. and Modena, C. (2015), “Simplified seismic assessment of multi-span masonry arch bridges”, *Bull. Earthq. Eng.*, **13**, 2329-2646.
Zampieri, P., Zanini, M.A., Faleschini, F., Hofer, L. and Pellegrino, C. (2017), “Failure analysis of masonry arch bridges subject to local pier scour”, *Eng. Fail. Anal.*, **79**, 371-378.

AT